CrossMark

Microstructure of as-extruded 7136 aluminum alloy and its evolution during solution treatment

Yun-Qiang Fan* , **Kai Wen, Zhi-Hui Li, Xi-Wu Li, Yong-An Zhang, Bai-Qing Xiong, Jian-Xin Xie**

Abstract With the aid of scanning electron microscopy (SEM), energy-dispersive spectroscopy (EDS), X-ray diffraction (XRD), differential scanning calorimetry (DSC) analysis and electron backscatter diffraction (EBSD), the microstructure of the alloy in as-extruded state and various solution-treated states was investigated. The results indicate that second phase of the as-extruded 7136 aluminum alloy mainly consists of $Mg(Zn, Cu, Al)_2$ and Fe-rich phases. The $Mg(Zn, Cu, Al)_2$ phase directly dissolves into the matrix during solution treatment with various solution temperatures. After solution treated at 475 °C for 1 h, $Mg(Zn, Cu, Al)_2$ phases are dissolved into the matrix, while Fe-rich phases still exist. Fe-rich phases could not dissolve into the matrix by prolonging solution time. The mechanical property test and EBSD observation show that two-stage solution treatment makes no significant improvement in mechanical properties and recrystallization of the alloy. The optimized solution treatment parameter is chosen as 475 °C/1 h.

Keywords 7136 Aluminum alloy; Microstructure; Solution treatment; Tensile property

Y.-Q. Fan*, K. Wen, Z.-H. Li, X.-W. Li, Y.-A. Zhang, B.-Q. Xiong
State Key Laboratory of Nonferrous Metals and Processes, General Research Institute for Nonferrous Metals, Beijing 100088, China
e-mail: fanyunqianglunwen@163.com

Y.-Q. Fan, J.-X. Xie
State Key Laboratory for Advanced Metals and Materials, University of Science and Technology Beijing, Beijing 100083, China

1 Introduction

The Al–Zn–Mg–Cu alloy plates are extensively used in the commercial aircraft structures as well as various critical military vehicles due to their excellent mechanical properties developed during the age-hardening process, like high strength-to-weight ratio, fracture toughness and stress corrosion cracking (SCC) resistance [1–10]. With the development of the aviation industry, researches on Al–Zn–Mg–Cu alloys have been focused on higher strength level, which mean higher degree of alloying and more reasonable design of the major alloying elements [11–13]. In recent years, several high-alloying aluminum alloys were registered and applied in the industries. Among them, the 7136 aluminum alloy is a representation [14–16].

It is well known that solution treatment is a key step for Al–Zn–Mg–Cu alloys to get excellent overall performance [17–21]. During the solution treatment, soluble phases can be re-dissolved into the matrix to form supersaturated solid solution, which prepares for subsequent aging treatment. At a higher solution temperature, soluble phases can re-dissolve more sufficiently. However, for the single-stage solution treatment, the solution temperature should be below the incipient melting point for $Mg(Zn, Cu, Al)_2$ phase. Otherwise, the alloy may be over-burnt, which is detrimental to the mechanical performance. Besides, a solution process at high temperatures led to severe recrystallization and decrease in the strength, toughness, and even resistance to corrosion of the aged materials [22, 23]. Hence, to avoid severe recrystallization and get good overall performance after aging treatments, a preferential solution treatment regime should choose relatively low temperature on the basis of ensuring the re-dissolution of the soluble phase. So it is necessary to study the

constituents in the as-extruded microstructure and the evolution during solution treatment.

There are many researches aiming at solution treatment of Al–Zn–Mg–Cu alloys [24–30]. With respect to the 7136 aluminum alloy, the as-cast and as-homogenized microstructures have been investigated [31]. However, the study on microstructure in the as-extruded 7136 aluminum alloy and its evolution during solution treatment is still very limited. In the present work, the constituents in the as-extruded microstructure and microstructural evolution during solution treatment were studied. The aim is to get an elementary understanding of the as-extruded constituents and their dissolution during solution treatment. Also, this will be helpful for the processing optimization for the alloy products during fabrication.

2 Experimental

The present study was carried out on the 25-mm-thick hot extruded Al–Zn–Mg–Cu alloy plate with chemical composition of Al–9.0Zn–2.0Mg–2.0Cu–0.14Zr (wt%). Solution treatments were conducted in air using a resistance heated box furnace with forced air convection. The melting temperature associated with constituent particles in the as-cast specimen was measured by differential scanning calorimetry (DSC, NETZSCH STA 409C/CD) instrument with a heating rate of 10 K·min^{-1} ranging from room temperature to 550 °C. DSC analysis was also performed on pure Al (99.999%) disks for temperature calibration to ensure the reliability of the measured data. The morphology of the residual phase was examined on scanning electron microscope (SEM, JEOL JSM 7001F). The second-phase particles were identified by energy-dispersive spectrometry (EDS) to quantitatively evaluate the dissolution of constituent particles. SEM images were taken at least at ten random sites for each sample. By using Image-Pro Plus software, the content of the remaining constituents in as-extruded and differently solution-treated samples was determined. The microstructural characterization was carried out by X-ray diffractometer (XRD, Rigaku D/Max 2500) with a step of 0.5°. The conductivity of the alloy at different conditions

was measured by a WD-Z eddy current conductivity meter with at least at five random sites for each sample. The recrystallization fraction was measured by electron backscatter diffraction (EBSD) on a JEOL JSM 7001F field emission scanning electron microscopy, and the images were taken at least at five random sites for each sample.

3 Results and discussion

3.1 Observation of as-extruded microstructure

The microstructure of the extruded Al–Zn–Mg–Cu alloy plate is shown in Fig. 1. It can be observed that a number of coarse second-phase particles distribute along the extruding direction. EDS analysis reveals that these second particles are Mg(Zn, Cu, Al)$_2$ phase and Fe-rich phase (Table 1). Large amounts of fine white phase are distributed homogenously in the matrix. According to EDS results, they are also Mg(Zn, Cu, Al)$_2$ phases. XRD pattern of the extruded 7136 alloy (Fig. 2) also proves that the primary phases are α(Al) and the phases with crystal structure of MgZn$_2$. Most second-phase particles are expected to be dissolved into the matrix by the solution treatment. However, the high temperature of the solution treatment inevitably increases recrystallization proportion. Therefore, it is necessary to optimize the solution treatment.

Table 1 EDS results of second-phase particles of extruded alloy plate in Fig. 1b (at%)

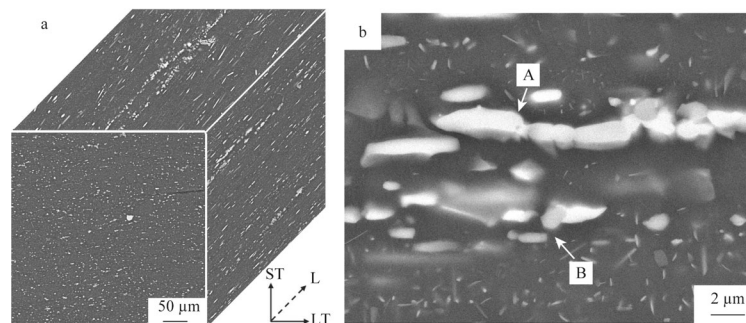| Points	Al	Zn	Mg	Cu	Fe
A	66.80	15.52	11.03	6.65	–
B	77.37	3.53	3.26	11.11	4.73

Fig. 1 SEM images of second-phase particles of extruded alloy plate: **a** 3D image of alloy, **b** phases on LS direction (L, LT and ST being longitudinal, long-transverse and short-transverse directions, respectively)
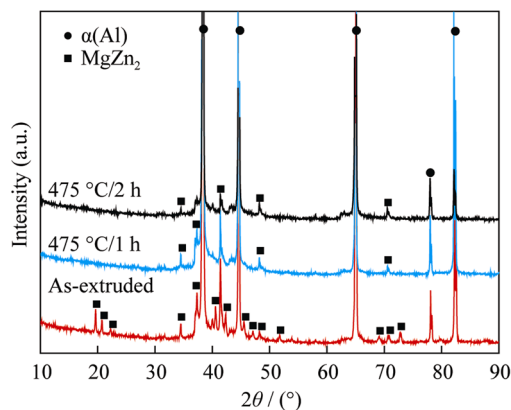
Fig. 2 XRD pattern of as-extruded, 475 °C/1 h and 475 °C/2 h alloys

3.2 DSC analysis of as-extruded alloy

DSC curve of as-extruded 7136 alloy is shown in Fig. 3. It could be clearly seen that the inflection point is 473.8 °C. The study by Xu et al. [21] declared that this temperature could be considered as the melting temperature of Mg(Zn, Cu, Al)$_2$ phase. From the perspective of experiment and engineering application, it is not appropriate to directly choose this temperature as the melting temperature of Mg(Zn, Cu, Al)$_2$ phase. The result deduced from DSC is a reference of temperature range. Under the influence of heating environment, heating rate, etc., the final re-dissolution of Mg(Zn, Cu, Al)$_2$ phase is not necessarily the measurement result of DSC. That means the DSC is not the only basis for temperature selection. The final temperature selection needs to do experiment around it to obtain applicable temperature.

3.3 Dissolution of constituent particles treated by various temperatures for 2 h

The solution treatment procedures are listed in Table 2. The typical micrographs of the alloy after solution treatment at different conditions are shown in Fig. 4. Mg(Zn,

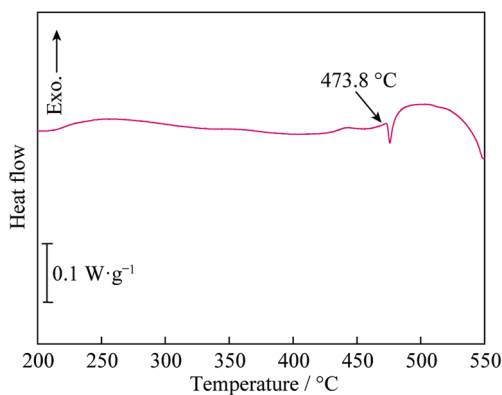**Table 2** Solution treatment schedules of extruded 7136 alloy plate

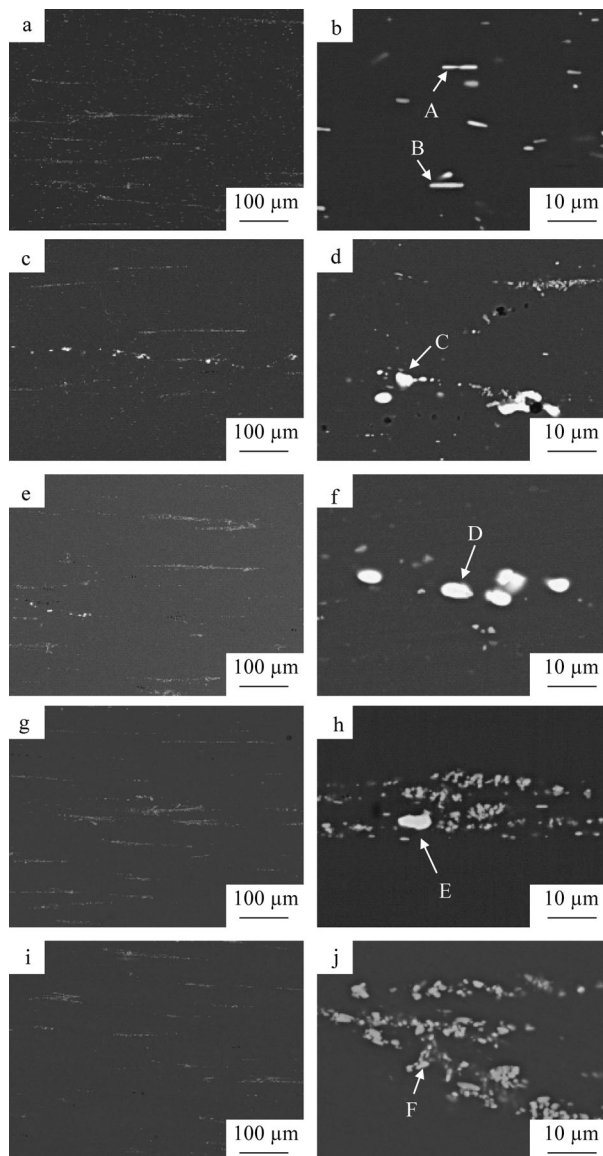| Samples	Solution treatment temperature/°C	Time/h
SHT450	450	2
SHT460	460	2
SHT465	465	2
SHT470	470	2
SHT475	475	2

Fig. 4 Typical SEM images of alloys after solution treated at different conditions: **a**, **b** SHT450, **c**, **d** SHT460, **e**, **f** SHT465, **g**, **h** SHT470 and **i**, **j** SHT475

Cu, Al)$_2$ phase is observed by EDS in Table 3 in SHT450, SHT460, SHT465 and SHT470 samples (Fig. 4a–g). Only Fe-rich phase is observed in the microstructure of SHT475 samples. It is necessary to note that Fe-rich phase is also


Fig. 3 DSC curve of as-extruded alloy

Table 3 EDS analysis of constituent phases in Fig. 4 (at%)

Phases	Al	Zn	Mg	Cu	Fe
A	72.44	10.09	11.69	5.78	–
B	69.16	10.57	13.78	6.49	–
C	28.09	23.19	32.11	16.61	–
D	41.39	18.44	26.73	13.44	–
E	48.95	17.80	20.26	12.99	–
F	80.48	–	1.87	12.15	5.50

observed in SHT450, SHT460, SHT465 and SHT470 samples, which is just not marked in the micrographs. It can be obviously seen that SHT samples treated at high temperatures possess less residual phases. In general, compared to the alloy extruded plate, the fine secondary phase particles are dissolved into the matrix of SHT samples.

The conductivity of the alloy at different conditions was also measured, as shown in Fig. 5. Typically, the conductivity was used to indicate the supersaturation level of alloys. Compared to that of as-extruded samples, the conductivity of SHT samples exhibits a significant decrement. Besides, the conductivity decreases with solution temperature increasing for SHT450, SHT460, SHT465 and SHT470 samples. That means a sustainable increment of the supersaturation of the matrix. Namely, the second-phase dissolution occurs all the time. This is in accordance with SEM observation. It is noted that the conductivity of SHT475 sample has no significant difference with that of SHT470 sample. This can be explained that too few $Mg(Zn, Cu, Al)_2$ phases remain in SHT470 sample so that their dissolution makes no significant change in conductivity.

In order to quantitatively analyze phase dissolution, the content of the second-phase particles treated with different conditions was statistically measured, as shown in Fig. 6. The results show that solution treatments have a significant
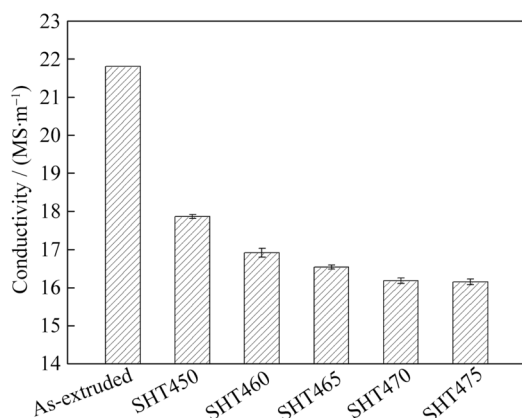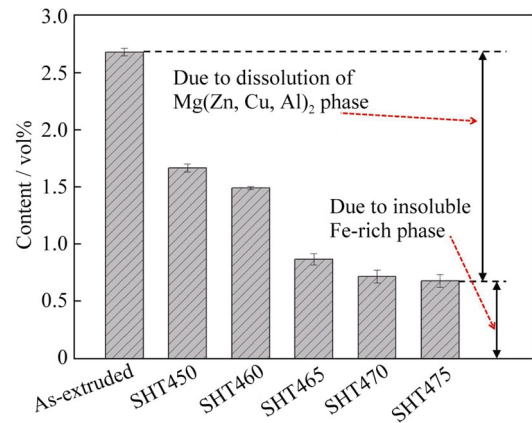
Fig. 6 Content of second-phase particles of alloys after solution treatment at different temperatures

effect on phase dissolution. After 2 h holding at 450 °C, the content of constituent particles in the alloy drops rapidly from 2.68 vol% to 1.67 vol%. The content of residual phases decreases with solution temperature increasing for SHT samples. The content of residual phases in SHT475 sample is 0.68 vol%. Correspondingly, only Fe-rich phase is observed, which is quite stable during solution treatment. Needless to say, it means that the contents of Fe-rich phase and $Mg(Zn, Cu, Al)_2$ phase are, respectively, about 0.68 vol% and 2.00 vol%.

3.4 Dissolution of constituent particles treated at 475 °C for various time

A further investigation on various solution time at 475 °C was conducted, and micrographs of the alloy after solution treatment are shown in Fig. 7. EDS analysis indicates that no $Mg(Zn, Cu, Al)_2$ phase exists in these conditions and only Fe-rich phase remains. This result is in good agreement with XRD analysis in Fig. 2.

At present, there is no significant difference among these conditions on the perspective of phase dissolution, so the mechanical properties of the alloy at different solution treatments followed T6 aging treatment were measured, as shown in Fig. 8. It is noted that no obvious distinction exists in ultimate tensile strength, while yield strength treated at 475 °C/1 h possesses an advantage. Hence, 475 °C/1 h is a preferential solution treatment parameter for single-stage solid solution.

3.5 Further exploration on double-stage solution treatment

Generally speaking, the adoption of double-stage solution treatment aims to decrease the recrystallization fraction of the alloy. In the present study, the preferential single
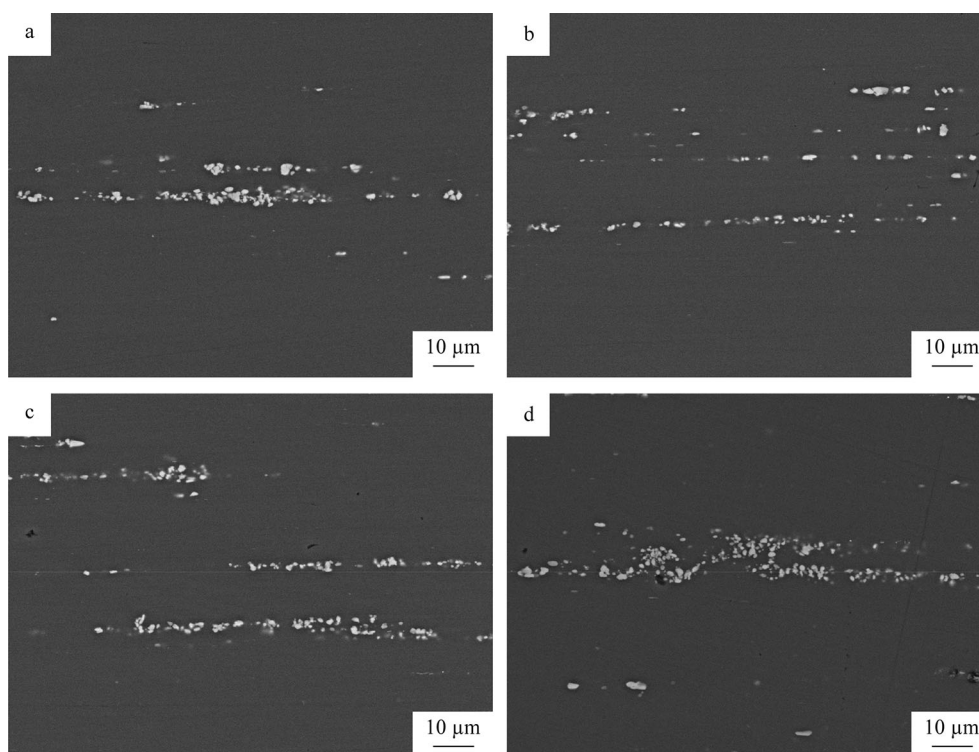

Fig. 5 Conductivity of alloys at different conditions

Fig. 7 Typical SEM images of alloys after solution treated at 475 °C for various time: **a** 0.5 h, **b** 1.0 h, **c** 1.5 h and **d** 2.0 h
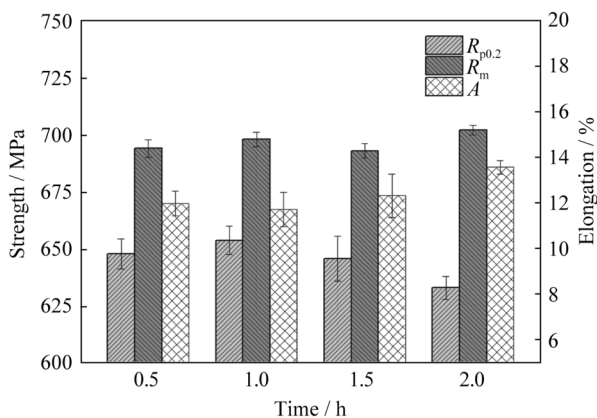

Fig. 8 Mechanical properties of alloys (in T6 condition) after solution treated at 475 °C for various time ($R_{p0.2}$, R_m and A being yield strength, ultimate tensile strength and elongation, respectively)

solution treatment ensures excellent Mg(Zn, Cu, Al)$_2$ phase dissolution. Hence, double-stage solution treatment focuses on the decrement of recrystallization fraction. According to other scholar's research, 450 °C/2 h was chosen as the first-stage solution treatment. Usually, recrystallization grains own high-angle grain boundaries, so statistical results of high-angle grain boundaries by EBSD can approximately represent the degree of recrystallization. Table 4 shows mechanical properties (in T6 condition) and

recrystallization fraction after 475 °C/1 h and 450 °C/2 h + 475 °C/(1, 2) h treatments.

It indicates that the double-stage solution treatment owes a slightly higher-angle grain boundary fraction than 475 °C/1 h treatment and makes no significant improvement in mechanical properties. That means recrystallization fraction possesses no remarkable difference between them and the first period of double-stage solution treatment has no obvious influence on recrystallization. Apparently, the preferential single solution treatment can effectively release the deformation energy storage and it is not necessary to adopt double-stage solution treatment. EBSD maps of the alloy at as-extruded state and solution treated at 475 °C for 1 h are shown in Fig. 9. It can be seen that the high-angle grain boundary fraction of the samples solution treated at 475 °C/1 h has no obvious difference with that of as-extruded samples. That means the single-stage solution treatment regime has a relatively satisfying control on recrystallization degree. Hence, considering the simplicity of operation, 475 °C/1 h is chosen as the optimized solution treatment parameter.

Besides, in order to reveal the microstructure of the alloy, the bright-field TEM (BF-TEM) images of the alloy treated by solution treatment of 475 °C/1 h and T6 aging treatment are shown in Fig. 10. It is found that fine

Table 4 Mechanical properties and recrystallization fraction of alloy (T6 condition) after several solution treatments

SHT schedules	Yield strength/MPa	Ultimate tensile strength/MPa	Elongation/%	High-angle grain boundary content/%
475 °C/1 h	654	698	11.7	40.8
450 °C/2 h + 475 °C/1 h	655	697	12.2	43.1
450 °C/2 h + 475 °C/2 h	656	696	12.3	45.5
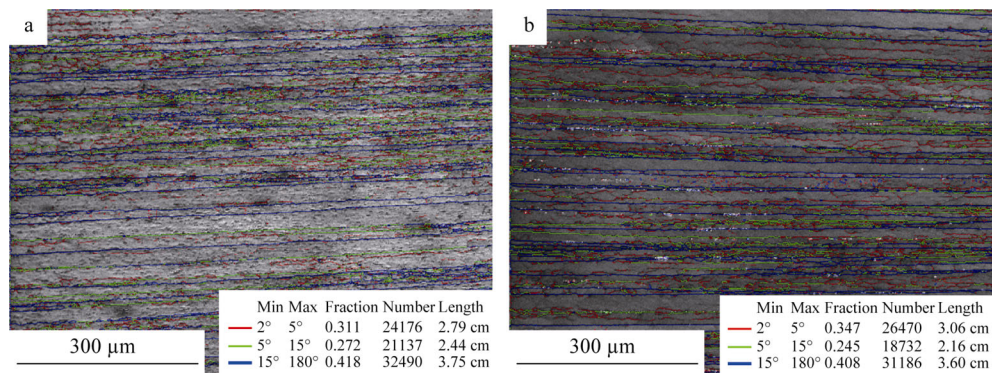
Fig. 9 Crystallographic EDSB maps and observation of alloy **a** at as-extruded state and **b** after solution treated at 475 °C for 1 h. Min and max being minimum and maximum rotation angle, respectively; fraction being proportion of rotation angles belonging to this interval; number being sum of collected rotation angles; length being average length of collected grain boundaries
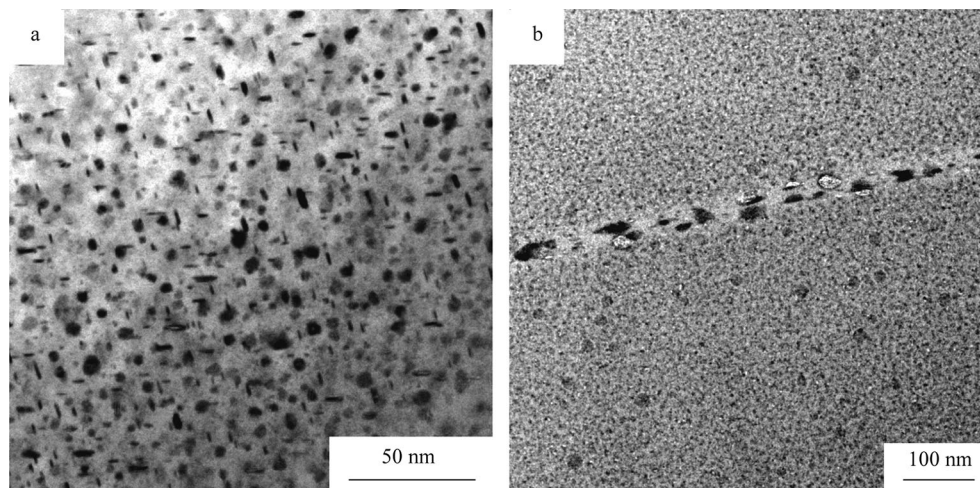
Fig. 10 BF-TEM images of alloy after solution treated by 475 °C/1 h and then aged under T6 condition: **a** matrix precipitates and **b** grain boundary precipitates

precipitates exist in the matrix and the grain boundary shows a continuous trend.

4 Conclusion

The second phases in the as-extruded microstructure mainly contain $Mg(Zn, Cu, Al)_2$ and Fe-rich phases, and their contents are 2.00 and 0.68 vol%, respectively. The $Mg(Zn, Cu, Al)_2$ phase directly dissolves into matrix during solution treatment. As solution temperature increases, the amount of residual $Mg(Zn, Cu, Al)_2$ phase decreases. This is in consistent with the change of conductivity. The Fe-rich phase has no obvious change after solution treatment. Double-stage solution treatment has no significant improvement on mechanical properties and recrystallization, and the optimized solution treatment parameter is 475 °C/1 h.

References

[1] Dursun T, Soutis C. Recent developments in advanced aircraft aluminium alloys. Mater Des. 2014;56:862.

[2] Wang X, Guo M, Cao L. Effect of heating rate on mechanical property, microstructure and texture evolution of Al–Mg–Si–Cu alloy during solution treatment. Mater Sci Eng A. 2015; 621:8.

[3] Mazibuko NE, Curle UA. Effect of solution heat treatment time on a rheocast Al–Zn–Mg–Cu alloy. Mater Sci Forum. 2011; 690:15.

[4] Liu Y, Jiang D, Xie W. Solidification phases and their evolution during homogenization of a DC cast Al–8.35Zn–2.5Mg–2.25Cu alloy. Mater Charact. 2014;93:173.

[5] Fan X, Jiang D, Meng Q. The microstructural evolution of an Al–Zn–Mg–Cu alloy during homogenization. Mater Lett. 2011; 60(12):1475.

[6] Liu Y, Jiang D, Li B. Heating aging behavior of Al–8.35Zn–2.5 Mg–2.25Cu alloy. Mater Des. 2014;60:116.

[7] Rometsch PA, Zhang Y, Knight S. Heat treatment of 7xxx series aluminium alloys—some recent developments. Trans Nonferrous Met Soc China. 2014;24(7):2003.

[8] Yang XB, Chen JH, Liu JZ. A high-strength AlZnMg alloy hardened by the T-phase precipitates. J Alloys Compd. 2014; 610:69.

[9] Marlaud T, Deschamps A, Bley F. Influence of alloy composition and heat treatment on precipitate composition in Al–Zn–Mg–Cu alloys. Acta Mater. 2010;58(1):248.

[10] Reda Y, Abdel-Karim R, Elmahallawi I. Improvements in mechanical and stress corrosion cracking properties in Al-alloy 7075 via retrogression and reaging. Mater Sci Eng A. 2008; 485(1):468.

[11] Chen SY, Chen KH, Peng GS. Effect of quenching rate on microstructure and stress corrosion cracking of 7085 aluminum alloy. Trans Nonferrous Met Soc China. 2012;22(1):47.

[12] Wang HJ, Xu J, Kang YL. Study on inhomogeneous characteristics and optimize homogenization treatment parameter for large size DC ingots of Al–Zn–Mg–Cu alloys. J Alloys Compd. 2014;585:19.

[13] Lin JT, Zhang YA, Li XW. Thermodynamic calculation of high zinc-containing Al–Zn–Mg–Cu alloy. Trans Nonferrous Met Soc China. 2014;24(5):1481.

[14] AMS4415A. Aluminum alloy extrusions, 8.9Zn–2.2Cu–2.2 Mg–0.15Zr (7136-T76511, -T76510) solution heat treated, stress-relieved, straightened, and overaged. SAE Technical Paper, 2008.

[15] Miller WS, Zhuang L, Bottema J. Recent development in aluminium alloys for the automotive industry. Mater Sci Eng A. 2000;280(1):37.

[16] Han NM, Zhang XM, Liu SD. Effect of solution treatment on the strength and fracture toughness of aluminum alloy 7050. J Alloys Compd. 2011;509(10):4138.

[17] Wang GS, Zhao ZH, Zhang YH. Effects of solution treatment on microstructure and mechanical properties of Al–9.0Zn–2.8 Mg–2.5Cu–0.12Zr–0.0Sc alloy. Trans Nonferrous Met Soc China. 2013;23(9):2537.

[18] Fang HC, Chen KH, Chen X. Effect of Cr, Yb and Zr additions on localized corrosion of Al–Zn–Mg–Cu alloy. Corros Sci. 2009;51(12):2872.

[19] Deng YL, Wan L, Zhang Y. Evolution of microstructures and textures of 7050 Al alloy hot-rolled plate during staged solution heat-treatments. J Alloys Compd. 2010;498(1):88.

[20] Xu DK, Rometsch PA, Birbilis N. Improved solution treatment for an as-rolled Al–Zn–Mg–Cu alloy. Part I. Characterisation of constituent particles and overheating. Mater Sci Eng A. 2012;534:234.

[21] Xu DK, Rometsch PA, Birbilis N. Improved solution treatment for an as-rolled Al–Zn–Mg–Cu alloy. Part II. Microstructure and mechanical properties. Mater Sci Eng A. 2012;534:244.

[22] Luo J, Li MQ, Ma DW. Microstructure and mechanical properties of 7A09 aluminium alloy after isothermal compression and solution treatment. J Mater Process Technol. 2012;212(5): 1039.

[23] Andean N, Taheri AK. Physically based material model for evolution of stress–strain behavior of heat treatable aluminum alloys during solution heat treatment. Mater Des. 2010;31(1): 433.

[24] Askari-Paykani M, Meratian M, Shayan M. Effects of heat treatment parameters on misconstruction changes and corrosion behavior of Al 7075 alclad alloy. Anti Corros Methods Meter. 2012;59(5):231.

[25] Xu DK, Birbilis N, Rometsch PA. Effect of S-phase dissolution on the corrosion and stress corrosion cracking of an as-rolled Al–Zn–Mg–Cu alloy. Corrosion. 2012;68(3):1.

[26] Yang XB, Chen JH, Liu JZ. Spherical constituent particles formed by a multistage solution treatment in Al–Zn–Mg–Cu alloys. Mater Charact. 2013;83:79.

[27] Li P, Xiong B, Zhang Y. Temperature variation and solution treatment of high strength AA7050. Trans Nonferrous Met Soc China. 2012;22(3):546.

[28] Chen K, Liu H, Zhang Z. The improvement of constituent dissolution and mechanical properties of 7055 aluminum alloy by stepped heat treatments. J Mater Process Technol. 2003; 142(1):190.

[29] Li G, Zhao N, Liu T. Effect of Sc/Zr ratio on the microstructure and mechanical properties of new type of Al–Zn–Mg–Sc–Zr alloys. Mater Sci Eng A. 2014;617:219.

[30] Anjabin N, Taheri AK. Physically based material model for evolution of stress–strain behavior of heat treatable aluminum alloys during solution heat treatment. Mater Des. 2010;31(1): 433.

[31] Li ZH, Zhang YA, Xiong BQ, Fan YQ, Li XW, Liu HW, Wang F, Zhu RR. Investigation on microstructure in as-cast aluminum alloy 7136 and its evolution during homogenization. In: 8 Pacific Rim International Congress on Advanced Materials and Processing, Waikoloa; 2013. 1299.